Investigations on cogging torque mitigation techniques of transverse flux motor for direct drive low-speed spacecraft applications

Ravichandran MH[1], Venkatakirthiga MURALI[2,*], Haridas TR[1]
[1]ISRO Inertial Systems Unit, Trivandrum, India
[2]Department of Electrical and Electronics Engineering, National Institute of Technology, Tiruchirapalli, India

Abstract: The transverse flux motor (TFM) is an ideal choice for direct drive high torque applications owing to its proven higher torque density compared to the radial flux and axial flux motors. TFM motors have several merits to be used for spacecraft applications, considering the everlasting demand of the industry for reduction in power and mass. This paper investigates the various cogging torque mitigation techniques for transverse flux motor to be effectively used as the drive motor for precise position control spacecraft requirement. The paper discusses the basic design variables of surface mounted TFM (SM-TFM) that are to be considered for minimizing the cogging torque. The effectiveness of cogging torque mitigation techniques are presented for two cases of SM-TFM, one with maximum cogging torque and the other with minimum cogging torque. The different torque ripple minimization techniques studied include skewing of rotor poles, notching of the stator poles, introduction of asymmetry in the stator structure, provision of wedges by the side of poles, segmentation of the magnets and introduction of shunt. The effectiveness of these cogging torque mitigation techniques is studied on two hardware variants of the TFM, one with the modified stator having shunt and the other with the modified rotor having low remanence permanent magnet. The TFM with a shunted stator is effective in torque ripple reduction in addition to the improvements in electromagnetic torque.

Key words: TFM, electromagnetic torque, cogging torque, torque ripple, skewing, asymmetry, notch and shunt

1. Introduction

The most important design consideration in the choice of low-speed high-performance torque motors for spacecraft applications is to obtain high torque density and efficiency and to minimize the torque ripple, and its related harmonics [1]. The presence of cogging torque or detent torque in the drive motor for the mechanism should be kept as low as possible, else it might result in micro-vibrations. Micro-vibrations created by the cogging torque will be transmitted to the spacecraft, which in turn affect the platform stability of the agile satellites [2]. The effects of torque ripple are undesirable in demanding spacecraft applications which require positional accuracy of less than a few arc second [3]. Torque ripples lead to speed oscillations which cause deterioration in the performance. They also excite resonances in the mechanical portion of the drive system, producing acoustic noise.

1.1. Transverse flux motor

The TFM was first introduced and named by Weh in 1986. In a TFM, the electromagnetic force vector is perpendicular to the magnetic flux lines. In contrast, in standard or longitudinal flux motors, the electromagnetic

---

*Correspondence: mvkirthiga@nitt.edu

force vector is parallel to the magnetic flux lines. Higher torque density is the prominent attractive feature of TFM. As the electric and magnetic loadings are independent, the achievable power to total machine weight ratio for active rotor TFM ranges between 0.5–2.0 kW/kg compared to 0.24–0.8 kW/kg for conventional machines. The capability to design a TFM with a higher pole number makes it superior to the axial and radial flux motor for low-speed and high-torque applications. TFM is capable of producing very high torque per unit volume provided that pole number is high [4]. TFMs are classified based on the type of excitation, its electromagnetic configuration, and the construction feasibility. Surface-mounted TFM is the basic configuration of TFM, where the permanent magnets are mounted on the surface of the rotor. Transverse flux motor is gaining due popularity due to its high torque density, making it an ideal candidate for direct-drive, large-torque, low-speed aerospace applications [5–8]. The major disadvantages of TFM are construction complexity and manufacturing difficulty due to complex structure.

1.2. Cogging torque

The interaction of the stator pole and a permanent magnet in torque leads to the production of cogging torque [9]. For low-speed drive mechanisms, having lesser inertia, cogging torque affects the speed stability of the system significantly. The projecting poles in the rotor and stator make the effect predominant on the production of cogging torque in TFM. This reluctance torque can be minimized either by minimizing the change in the reluctance of airgap or by reducing the airgap flux density. Reduction of cogging torque in TFM is the major design criteria as it does not contribute to any useful torque and results in pulsating torque and torque ripple, particularly at light load and low speed. Various techniques for the minimization of cogging torque are detailed in [10]. The cogging torque reduction techniques like the introduction of skewing, notches and effect of pole-arc to pole-pitch ratio is given in [11]. The effect of pole number on electromagnetic torque and cogging torque is given in [12]. The effect of magnet shape on cogging torque is elaborated in [13]. Effect of skewing and step skewing are given in [14–17]. The use of alternate magnet pole-arcs is proposed in [18]. Symmetrical and asymmetrical shifts of the stators in TFMs are presented in [19] as a method of torque ripple reduction. The stator tooth shapes are also optimized to reduce cogging torque in [20]. Stator displacement of double-sided machine is given in [21, 22]. Cogging torque minimization of flux switching TFM is detailed in [23]. Other techniques like multi-level skewing is provided in [24] and Herringbone technique in [25]

The conventional cogging torque mitigation techniques used in brushless DC (BLDC), permanent magnet synchronous motor (PMSM) and switched reluctance motor (SRM) are extensively studied for SM-TFM. The objective of this paper is to study in detail these cogging torque mitigation techniques for SM-TFM and to make a comparative analysis to select a suitable technique that is capable of meeting the demands of maximum electromagnetic torque and minimum cogging torque and torque ripple. The influence of the basic parameters of the machine like the pole number, thickness of the airgap, the radial and axial thickness, and the remanence of the magnet was studied in detail to select the optimum value. The rotor and stator pole-arc are selected as the design variables and the parametric analysis of the same was carried out. Here two cases were identified one with maximum and the other with minimum cogging torque. The total stored electromagnetic energy in the airgap of the machine remains constant. Cogging torque shall be reduced by increasing the cogging torque pulsation in the airgap, thus by reducing its peak. Various cogging torque mitigation techniques like, effect of skewing, introduction of machine asymmetry, notches, wedges and shunt, segmentation of magnets were studied in detail for these two cases. Experimental validation of the machine was carried out to study the effect of pole number, shunting of stator and remanence of the permanent magnet.

TFM has complex magnetic field distribution and calls for 3-D finite element analysis (FEA). Commercially available FE software, Ansys Maxwell-3D was used to carry out the electromagnetic analysis. Section 2 gives the details of the influence of basic design parameters of TFM on cogging torque and the selection of cases based on design variables. Section 3 gives the study of various cogging torque mitigation techniques on the selected cases. Section 4 provides the realization details and the experimental validation of three variants of TFM and paper concludes with Section 5.

2. Influence and selection of design variables for cogging torque minimization

The SM-TFM under analysis has 14 rotor pole pairs as shown in Figure 1. Number of iteration for a FEA simulation is 20 and the error between subsequent iterations is 0.1%. After 20 passes, the number of tetrahedrons for the model is nearly 7 Lacs and the time elapsed for one simulation is 35 min.
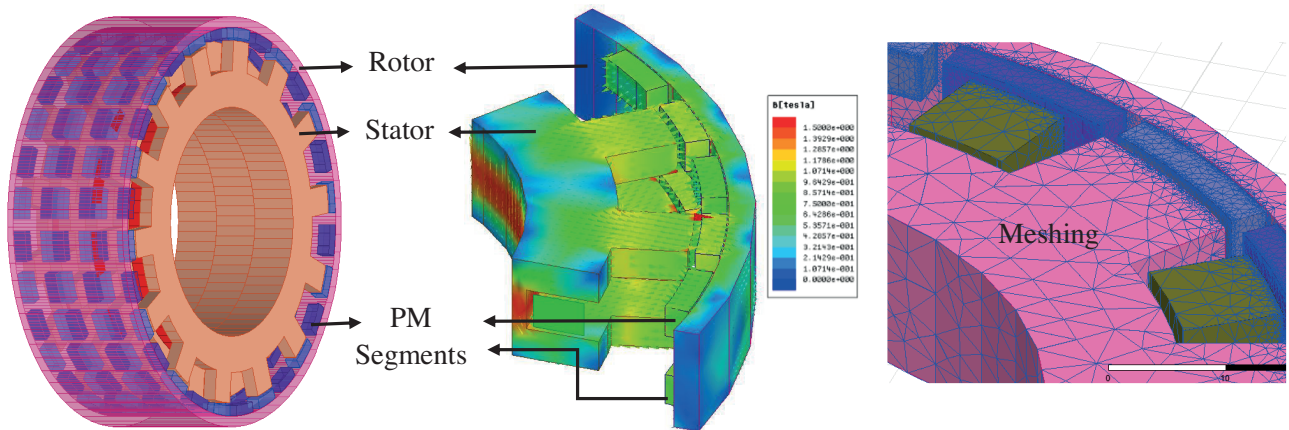

Figure 1. Solid model, flux distribution and meshing pattern of SM-TFM

The Stator and rotor pole-arc to pole-pitch ratio is 0.72 and 0.32, respectively. The radial thickness of the magnet is 4 mm and the axial thickness is 53% of the total thickness. The stator has 450 turns of copper wire and the excitation voltage is 42 V. The functional airgap between stator and rotor is 1 mm. The influence of basic parameters of TFM like pole number, the thickness of airgap, the axial and radial thickness of the magnet on cogging torque is studied on this SM-TFM. Pole-arc of stator and rotor are selected as the design variables, and two cases were identified for further analysis.

2.1. Influence of basic parameters of TFM on cogging torque

2.1.1. Effect of pole number.

The electromagnetic torque in TFM is directly proportional to the pole number in TFM. Leakage between the poles increases with the increase in the number of poles. This in effect reduces the useful torque. The results are tabulated in Table 1.

Table 1. Effect of pole number

Pole number	12	16	20	24	28	32	36
Avg electromagnetic torque (Nm)	0.80	0.98	1.12	1.26	1.35	1.35	1.44
Pk cogging torque (Nm)	0.05	0.01	0.07	0.19	0.02	0.02	0.03
Torque ripple (%)	33.8	42.7	62.7	48.9	52.4	57.9	58.7

Even though there is an increase in electromagnetic torque with the increase in the pole number, torque ripple also shows a considerable increase with the pole number. The peak cogging torque shows a variation in the pattern with the pole number.

2.1.2. Effect of air-gap

There exists a direct relationship between the torque produced by the motor and the air-gap thickness. Air-gap is varied from 0.4 mm to 1.6 mm and its effect on developed torque is shown in Figure 2. It is inferred that there exists a linear relationship between the thickness of the air-gap and the electromagnetic torque whereas it is inverse-square for cogging torque. Cogging torque can be reduced with larger airgap. Higher excitation will compensate the corresponding reduction in electromagnetic torque as magnetic and electric loading has no inter-relationship in TFM.

2.1.3. Effect of remanence (Br) of permanent magnet

The remanence of the PM is varied from 10% to 100% and its effect on the performance parameters of TFM is shown in Figure 2. It is inferred that electromagnetic torque, which is proportional to airgap flux density, varies linearly with the remanence. With 30% reduction in the remanence of PM, there is 23% reduction in electromagnetic torque, whereas cogging torque is reduced by 40%.
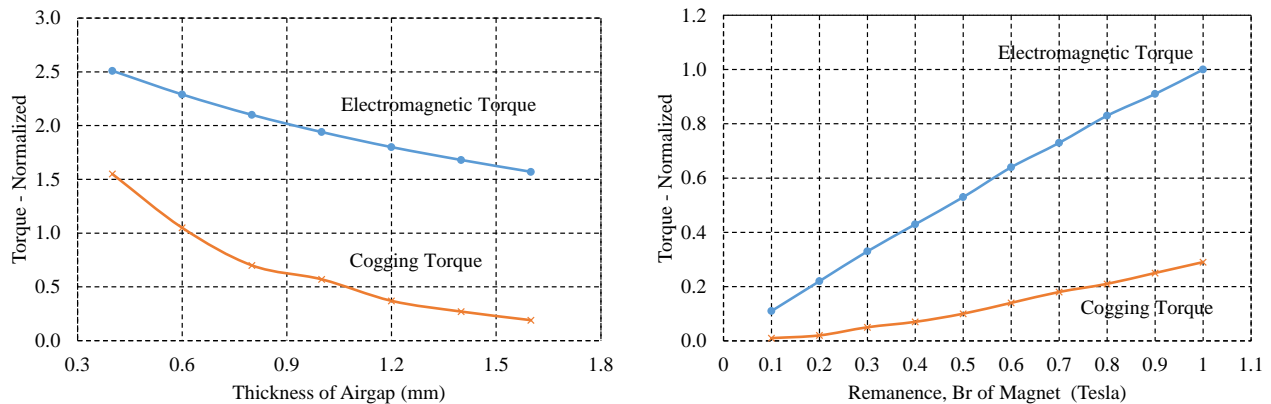

Figure 2. Effect of airgap thickness and remanence of magnet on electromagnetic torque and cogging torque of SM-TFM.

2.1.4. Effect of radial and axial thickness of the magnet

The role of radial and axial thickness of permanent magnet (PM) on developed torque is studied. In transverse flux machines, the inactive magnets increase the leakage flux of the machine and hence the useful torque. Cogging and electromagnetic torque variation with the change in the radial and axial thickness of the magnet are shown in Figure 3. It is found that when the magnet radial thickness is 57% of the stator pole thickness, the motor delivers maximum electromagnetic torque and cogging torque is 0.17 times the electromagnetic torque. The electromagnetic torque follows the inverse parabolic relationship and is maximum when the axial gap between the magnets is 53% of the total axial length, whereas cogging torque decreases in direct proportion with axial inter pole gap. With the change in the radial and axial thickness of the magnet, the magnet volume also changes and hence there is change in the mass of the magnet.
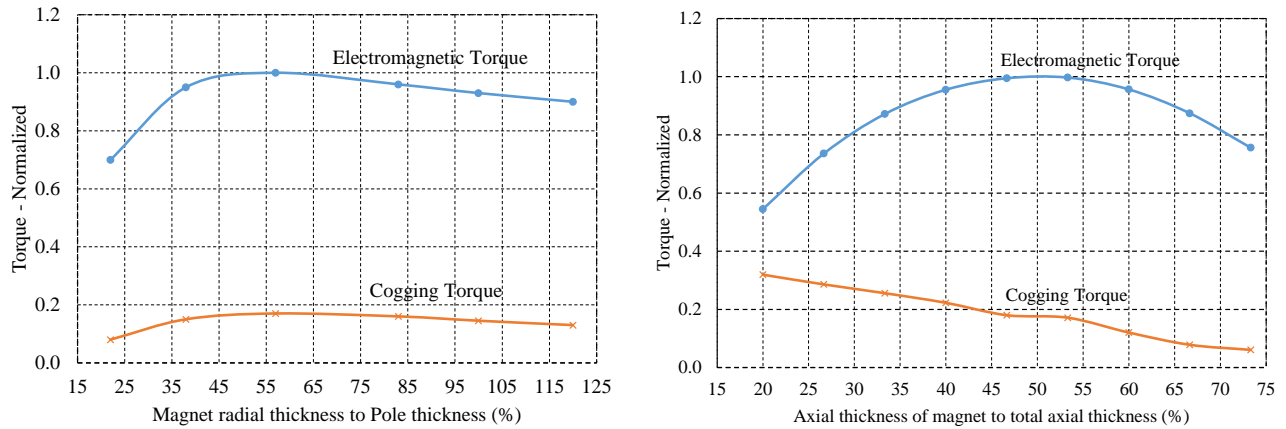
Figure 3. Effect of radial and axial thickness of magnet on electromagnetic torque and cogging torque of SM-TFM.

2.2. Selection of design variables – variation of pole arc

The pole-arc to the pole-pitch ratio (t/λ) of stator and rotor poles has a prominent effect on the developed torque of TFM. It affects the magnitude and the pattern of the developed torque. With the variation of pole-arc angle, the shape of Back EMF changes which in turn affects the average electromagnetic torque. Stator pole thickness variation also has a similar impact on the torque pattern as that of the rotor pole-pitch. Stator and rotor t/λ are selected as the design variables. The variation of the cogging and electromagnetic torque of TFM under analysis with the variation of rotor and stator t/λ is shown in Figure 4.
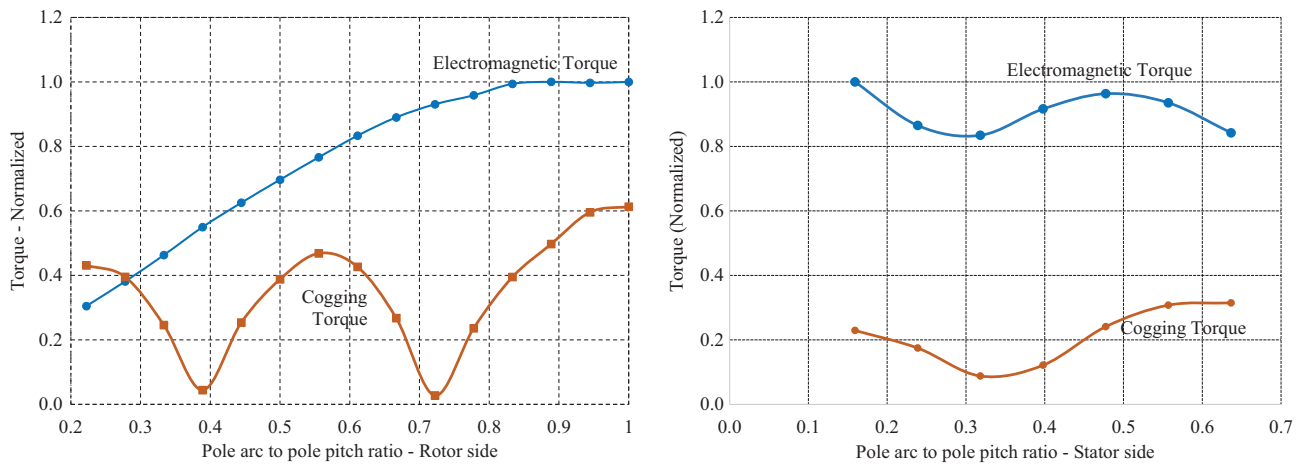

Figure 4. Effect of stator and rotor t/λ on developed torque

It is inferred that, there are two rotor t/λ where the cogging torque is minimum. The electromagnetic torque varies linearly till the second minimal point and flattens then after. Stator t/λ is not as significant as rotor t/λ as far as cogging torque is concerned. Parametric analysis with the variation of stator and rotor t/λ was carried out. Stator t/λ is varied from 21.6% to 64.9% and rotor t/λ is varied from 44.4% to 88.8%. The effect of these design variables on cogging torque, torque ripple and developed torque are tabulated in Table 2.

From the parametric analysis of the design variables, two cases were selected one with near minimum cogging torque (Case-1) and the other with near-maximum (Case-2). The details are tabulated in Table 3.

Table 2. Effect of design variables on cogging torque, developed torque and torque ripple of TFM.

Stator pole arc %	Rotor Pole-arc (%)														
	Cogging Torque (Nm)					Torque Ripple (%)					Dev Torque(Nm)				
	44.4	55.5	66.7	77.8	88.9	44.4	55.5	66.7	77.8	88.9	44.4	55.5	66.7	77.8	88.9
21.6	0.46	0.85	0.38	0.46	0.82	179	155	126	108	95	1.28	1.54	1.74	1.83	1.89
27.0	0.36	**0.08**	0.29	0.28	0.21	174	**125**	84	74	39	1.26	**1.58**	1.84	1.95	2.06
32.4	0.39	0.89	0.68	0.38	1.08	153	105	66	35	32	1.25	1.57	1.82	2.00	2.04
37.8	0.53	0.99	0.47	0.53	1.05	116	91	63	45	49	1.27	1.54	1.77	1.92	1.98
43.2	0.45	0.31	0.13	0.41	0.20	124	92	77	65	61	1.23	1.52	1.72	1.89	2.01
48.6	0.22	0.67	0.52	0.20	**0.80**	171	132	101	87	**62**	1.13	1.44	1.70	1.88	**2.02**
54.1	0.51	0.84	0.45	0.49	0.90	217	146	113	88	81	1.08	1.42	1.68	1.85	1.92
59.5	0.41	0.29	0.11	0.40	0.09	164	174	140	115	108	1.14	1.34	1.57	1.68	1.68
64.9	0.23	0.70	0.53	0.26	0.93	151	136	154	162	157	1.12	1.30	1.39	1.38	1.34

Table 3. Details of selected Case-1 and Case-2

Design Variables	Stator t/λ (%)	Rotor t/λ (%)	Cogging Torque (Nm)	Torque Ripple (%)	Developed Torque (Nm)
Case-1	27.0	55.5	0.08	125	1.58
Case-2	48.6	88.9	0.80	62	2.02

The other design data like pole pairs, airgap thickness, radial and axial thickness of magnet, windings and excitation voltage are as given in Section 2. The solid model and the developed torque of TFM for these two cases are shown in Figure 5. It is inferred that, compared to Case-2, in Case-1, cogging torque is less and torque ripple is more as the variation in electromagnetic torque is more. Even though cogging torque is the major contributor to torque ripple, here in TFM electromagnetic torque pattern also plays a role in the torque ripple. In both cases, cogging torque and torque ripple pose an inverse relationship. Even though the peak torque for the two cases are identical, the minimum developed torque for Case-1 is lesser than for Case-2. This led to an increase in the torque ripple in Case-1. To reduce torque ripple, the pattern of the developed torque also has to be modified in addition to the minimization of the cogging torque. From the flux pattern, it is inferred that the flux density at the stator pole for Case-2 is lesser than Case-1 because of the increase in volume.

3. Effect of cogging torque mitigation techniques

Here in this section, various cogging torque mitigation techniques are implemented on the identified two cases. The effect of the cogging torque mitigation techniques on developed torque and torque ripple are detailed.

3.1. Effect of skewing

The most common and basic method for the reduction of cogging torque is skewing. [10, 25]. Skewing is carried out either in the stator or rotor, continuously or in steps. Unlike PM machines, stator skewing will not add complexity to TFM. The effect of simple and stepped skewing was studied.
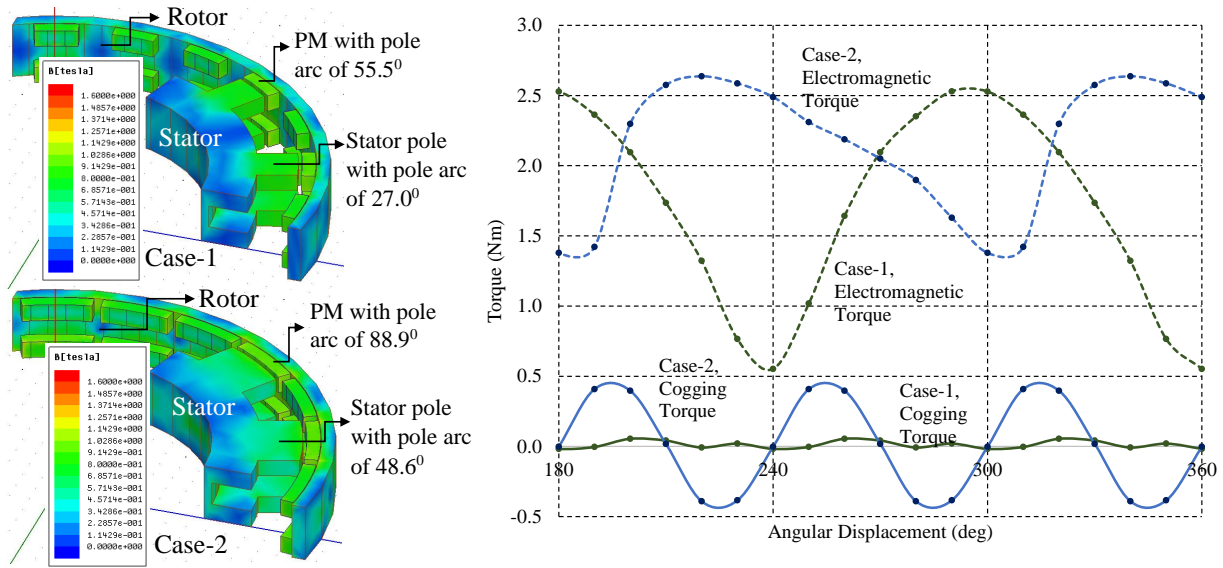
Figure 5. Solid model and the developed torque pattern of TFM - Case-1 and 2.

3.1.1. Simple skewing

Parametric analysis of the skew angle was carried out in both cases. The skew angle is varied to 100% of the pole-pitch. The solid model and the developed torque pattern with the change in the skew angle for both the cases are shown in Figure 6. It is inferred that, In Case-1, there is no appreciable reduction in the cogging torque till 50% of skew angle but increases drastically after half skew. There is a reduction in torque ripple till 50% of skew angle in this case. For Case-2, it is found that there exist two skew angles where the cogging torque is minimum. However, torque ripple increases with the increase in the skew angle and decreases beyond 80% of the skew angle. There is a reduction in the electromagnetic torque with the increase in the skew angle in both cases.
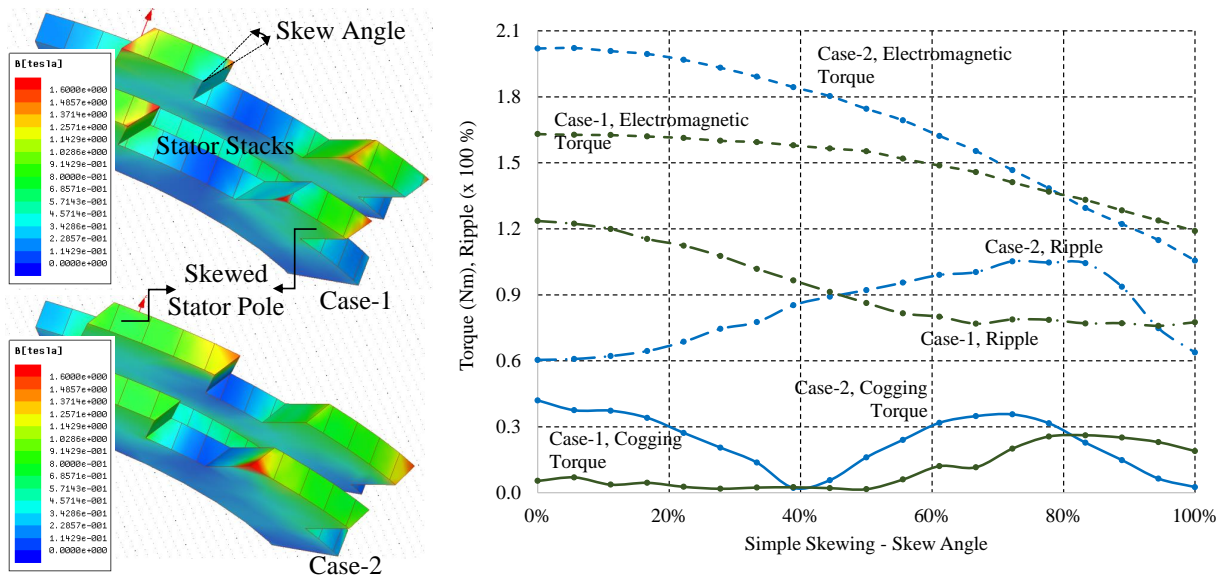

Figure 6. Solid model and the developed torque pattern of TFM with simple skewing - Case-1 and 2.

3.1.2. Stepped skewing

Even though the half or full skew of the stator eliminates the cogging torque, it possesses certain practical difficulties in manufacturing. This can be overcome by an alternative approach called stepped skewing. Here the skewing is done in discrete steps. This approach is studied in Case-1 and Case-2. The solid model and the developed torque pattern with stepped skew for both cases are shown in Figure 7. It is inferred that as in simple skewing, cogging torque and torque ripple follow the same pattern with the skew angle but with increased magnitude. With stepped skewing, there is a reduction in the electromagnetic torque in both cases than of simple skewing.
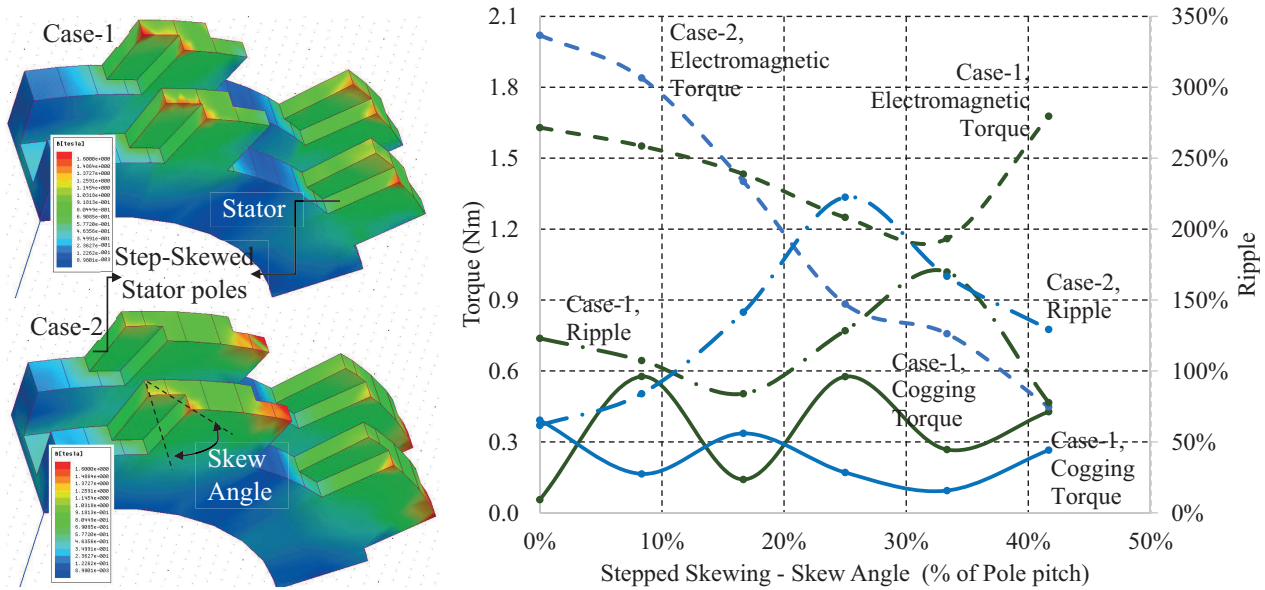

Figure 7. Solid model and the developed torque pattern of TFM with stepped skewing- Case-1 and 2.

Leakage flux analysis is carried out for this simple and stepped skewing. Leakage flux distribution patterns for both cases are identical and the leakage flux is relatively more at the outer surface, where there is no interaction of stator and rotor segments. In addition, it is found that for stepped skewing, the maximum leakage flux outside the motor was 15 Gauss (max) whereas it is 4 Gauss (max) for simple skewing.

3.2. Influence of machine asymmetry - pole shifting

There is a component in cogging torque, whose period is one half of the slot-pitch. All the rotor magnets are in phase and their sum contributes to the total cogging torque [26–28]. The introduction of asymmetry modifies its phase and thus reduces its sum and hence the cogging torque. The symmetry of the machine can be disturbed by using techniques like pole-shifting and pole-pairing. While most of the pole-pairing techniques disturb the symmetry, some of the techniques introduce more symmetry and lead to the unbalance of the rotor. Two types of pole-shifting (1. in the same stack, 2. in opposite stack) were adopted for both cases. The model is shown in Figure 8.

The angle between adjacent poles under the same stator stack is modified in pole-shifting (same-stack) type, and pole angle between opposite stacks is modified in pole-shifting (opposite-stack) type.

From the developed torque profile and pattern for both cases shown in Figure 9, it is found that pole shifting techniques are more effective in Case-2, where initial cogging torque is more. As pole shifting disturbs the machine's symmetry, there is a considerable reduction in developed torque for both cases with these two approaches. Even though the torque ripple is less for opposite stack pole shifting at a lesser shifting angle for Case-2, it rises beyond 15% of pole-pitch as partial portion of stator pole pair comes under the same polarity.
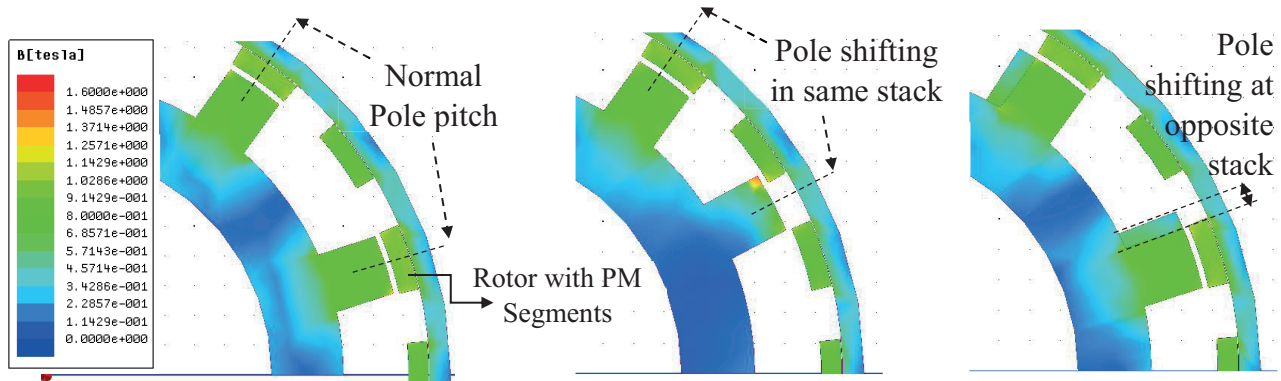

Figure 8. Flux distribution of TFM without and with pole shifting (same and opposite stack)- Case-1.
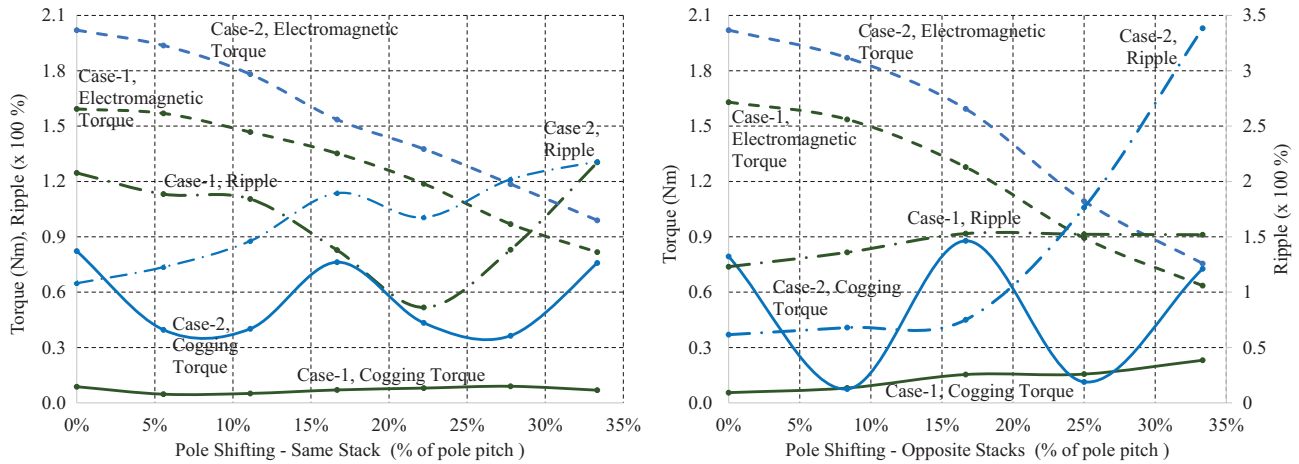

Figure 9. Effect of same and opposite stack pole shifting on the developed torque pattern of TFM - Case-1 and 2.

3.3. Notching of stator poles

In this technique, notches are provided in the stator pole. This acts as the additional tooth and increases the number of times the permanent magnet interacts with the tooth tips, thus increasing the frequency of the cogging torque [29]. As the energy in the airgap remains constant, the increase in the frequency decreases the peak amplitude of the cogging torque. Figure 10 shows the solid model of TFM with single and double notch for Case-1 and Case-2. It is seen that the tooth tip of the notches of stator pole with a double notch is experiencing higher flux density due to material reduction.

Parametric analysis is carried out with the change in the thickness and height of the notch for both cases. It is found that for both cases, the depth of the notch is not having a considerable effect on the performance

as there is no material saturation. Developed torque and torque profile patten for both cases are shown in Figure 11 and it is inferred that both single and double notch configurations are more effective for Case-2 in cogging torque reduction. Electromagnetic torque decreases considerably from the initial value in single notch configuration than in double notch, with the increase in the notch thickness for both cases.

In a single notch configuration, torque ripple decreases in Case-1 when the notch thickness is more than 50% of the pole thickness. In double notch configuration, cogging torque decreases in Case-2 when the notch thickness is more than 40% of the pole thickness.
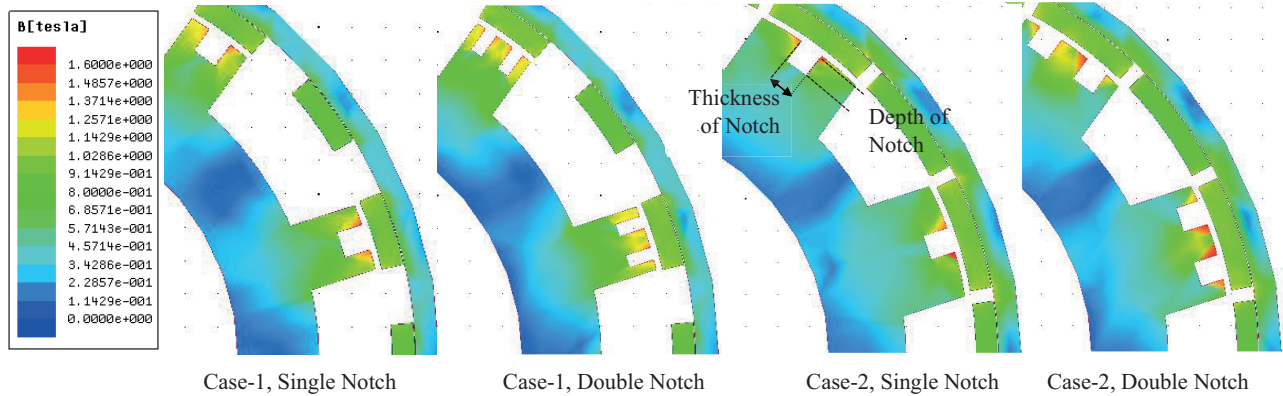

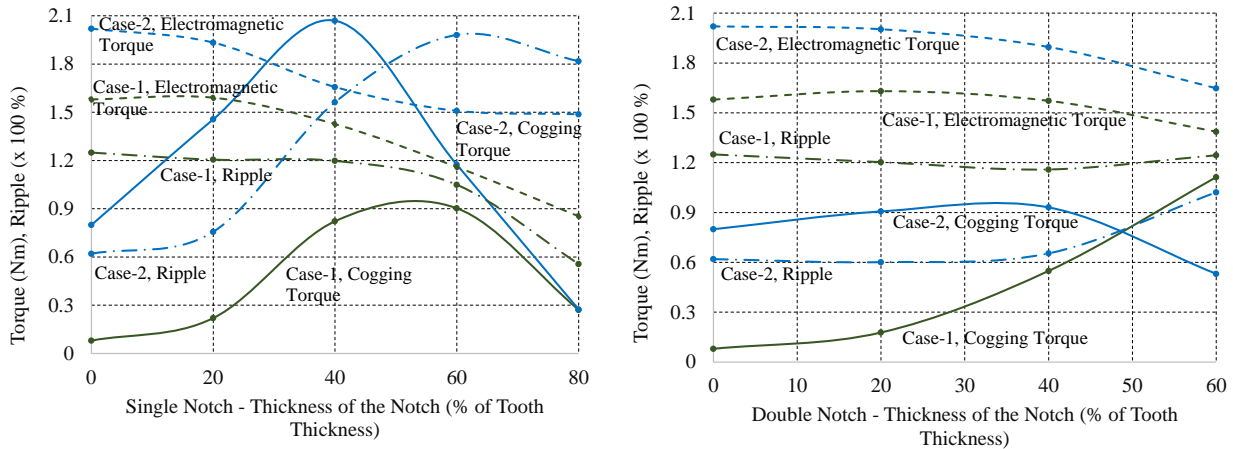Figure 10. Flux distribution of TFM with single and double notch - Case-1 and 2.

Figure 11. Developed torque pattern of TFM with single and double notch - Case-1 and 2.

3.4. Effect of wedge

The general cause of cogging torque is fringing flux produced just before the overlap of the stator and rotor teeth. The flux introduces torque variation [30] which can be overcome by modulating the fringing flux with the introduction of wedges at stator poles of TFM as shown in Figure 12.

Parametric analysis is carried out with the variation of height and depth of wedge. There is no appreciable change in the performance of the motor with the change in the height of the wedge as in the case of notching. Developed torque and torque profile patten for both cases are shown in Figure 12 with the increase in the depth of the wedge. It is inferred that wedges, which modulate fringing flux have minimum impact on electromagnetic

torque as it is produced by main flux. Wedging is more effective in Case-2 as the contact area for fringing flux is more and cogging torque is reduced by 76% when the wedge depth is 50% of the pole thickness.
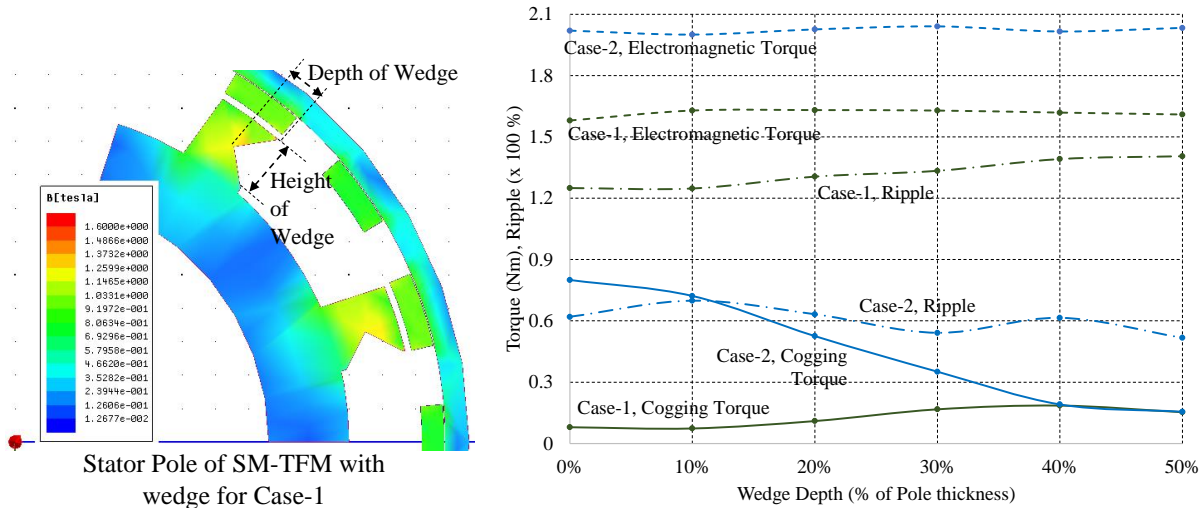

Figure 12. Flux distribution and developed torque pattern of TFM with wedge - Case-1 and 2.

3.5. Effect of magnet segmentation

For TFM with a lesser pole number, the magnet pole span will be large and will be realized in segments. Since these segments have the same relative positions as stator slots, their interaction with the slots of the stator has additive effect [31]. This additive effect can be broken by introducing asymmetry between segments. Figure 13 shows the flux distribution and the torque pattern of TFM with the variation of the gap between the segments for a 3 segmented model. From the flux plot, it is found that the magnetic flux density at stator and rotor core in this configuration is relatively lesser than that of other configurations, which is due to the reduction in the magnetic loading.
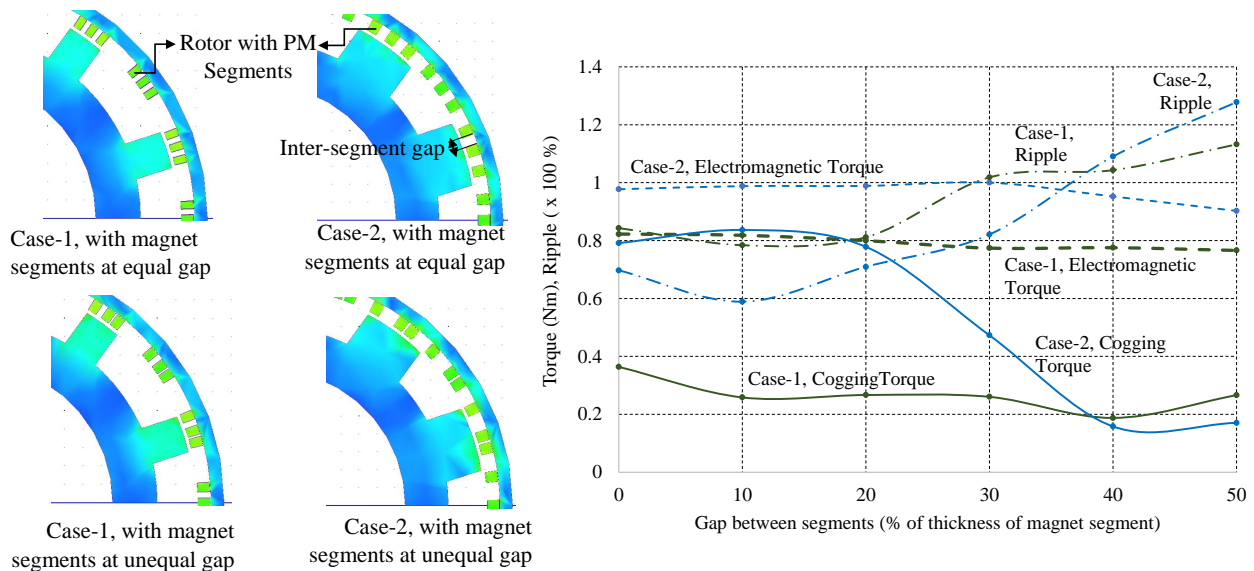

Figure 13. Flux distribution and developed torque pattern of TFM with magnet segmentation - Case-1 and 2.

Parametric analysis is carried out with the change in the thickness of segments and the gap between segments. From the torque pattern shown in Figure 13, it is inferred that even though the magnitude of electromagnetic torque is lower in both cases, which is due to the reduced magnetic loading, there is no appreciable change with the variation in the gap between the segments, as it is not modulating the main flux. Torque ripple shows an increasing trend for both cases. In Case-2, where the initial cogging torque is higher, it reduced up to 81% of the initial value, when the inter-segment gap is increased as it creates asymmetry.

3.6. Effect of shunt

In surface mounted TFM, active torque is produced only by half of the magnets as the number of stator poles is half of the rotor poles. Leakage flux produced by the other half of the magnets can be used to produce useful torque with the introduction of shunts. [32]. The shape of the shunt can be tapered or square and made of magnetic material placed between stator poles to use the flux produced by the inactive magnets. With the introduction of the shunt, the flux produced by the inactive magnets gets a closed path through it. Figure 14 shows the TFM with square and trapezoidal shunt for both cases. It is seen for the flux pattern that flux density at the bottom portion of the trapezoidal shunt is comparatively higher than that of with square shunt, which helps in the marginal improvement of the alignment torque in TFM with a trapezoidal shunt. The thickness and slant angle of the shunt are considered for the parametric analysis.

The effect of the slant angle on the performance of the motor is considerably less. Figure 15 shows the electromagnetic torque pattern and torque ripple for both cases of TFM with the square shunt and trapezoidal shunt (shunt angle is 25°) with the variation of the thickness of the shunt.
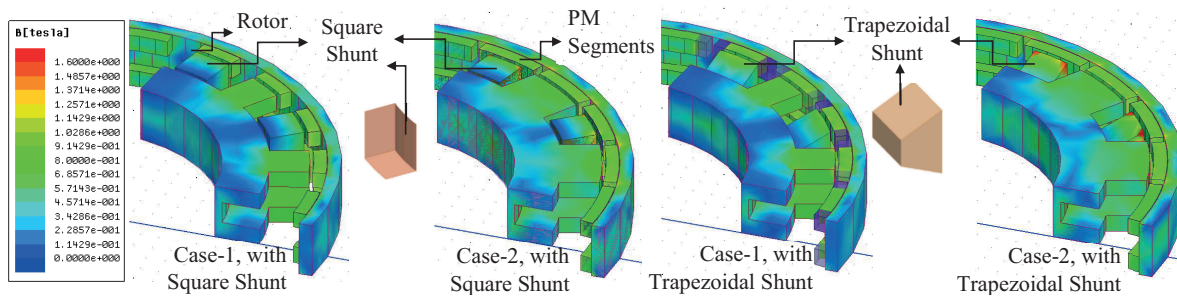

Figure 14. Solid model of TFM with square and trapezoidal shunt - Case-1 and 2.
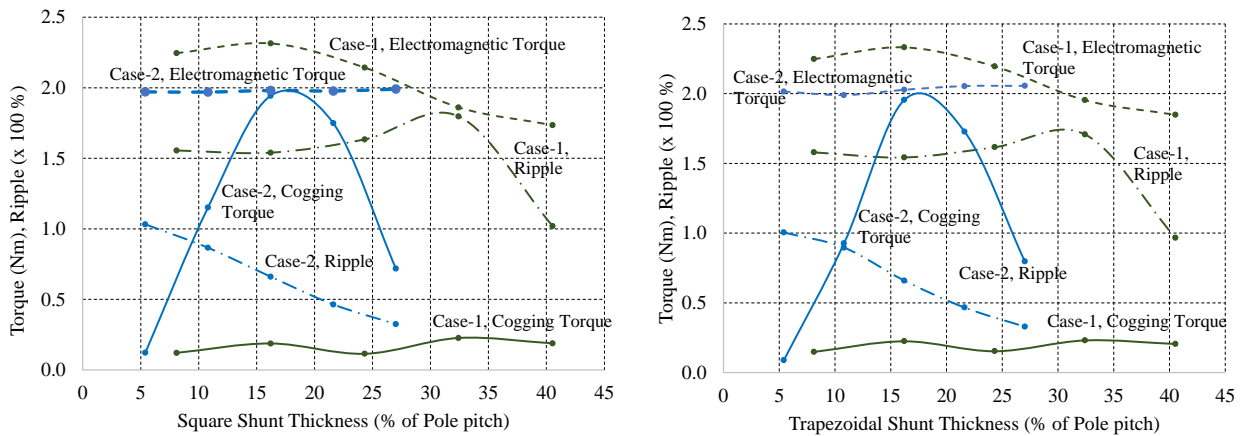

Figure 15. Developed torque of TFM with square and trapezoidal shunt - Case-1 and 2.

It is inferred that with the introduction of shunt, torque ripple reduces by 22% and 20% for Case-1 and Case-2, respectively, which is due to the improvement of the second half of the electromagnetic torque pattern. The comparison of the performance parameters of both cases of TFM under various cogging torque mitigation techniques is tabulated in Table 4. All the techniques have a considerable effect in Case-2, where the initial value of cogging torque is more. While Cogging torque decreases in Case-2 with mitigation techniques, torque ripple increases with all techniques except wedging. In Case-1, where initial cogging torque is more, there is no substantial reduction in the cogging torque, but a considerable reduction in the torque ripple.

Table 4. Comparison of various cogging torque mitigation techniques on the performance parameters of TFM.

Parameter	Case-1			Case-2		
	Cogging Torque (Norm)	Developed Torque (Norm)	Torque Ripple ((Norm)	Cogging Torque (Norm)	Developed Torque (Norm)	Torque Ripple (Norm)
01. Original	0.05	1.00	1.00	0.51	1.28	0.50
02. Skewing - Simple	0.02	0.92	0.86	0.04	1.17	0.68
03. Skewing - Multi	0.09	0.91	0.67	0.06	0.48	1.33
04. Notching - Single	0.17	0.54	0.45	0.17	0.94	1.46
05. Notching - Double	0.34	0.94	0.93	0.34	1.04	0.82
06. Pole shifting - Opposite	0.03	1.03	0.98	0.04	1.18	1.08
07. Pole shifting - Angle	0.03	0.99	0.91	0.25	1.23	0.59
08. Wedge	0.05	1.00	1.00	0.12	1.27	0.47
09. Magnet segmentation	0.16	0.53	0.63	0.09	0.60	0.87
10. Shunt - Square	0.08	1.09	0.82	0.08	1.25	0.82
11. Shunt - Trapezoidal	0.09	1.17	0.78	0.06	1.27	0.80

It is observed that both skewing techniques considerably reduce the cogging torque in Case-2 and torque ripple in Case-1, where their respective initial values are more. With the increase in the skewing angle, electromagnetic torque decreases. For Case-2, with the introduction of the wedge, there is a considerable reduction in cogging torque which was not observed in Case-1. With magnet segmentation, the total magnetic loading came down, which led to a decrease in electromagnetic torque in both cases. In Case-2, electromagnetic torque decreases and torque ripple increases with the implementation of cogging torque mitigation technique. Among all cases, the introduction of shunt has provided an added advantage of an increase in the electromagnetic torque in addition to the decrease in torque ripple with minimal increase in cogging torque for Case-1.

4. Experimental validation

To experimentally verify the effect of the basic parameters of TFM and the most suitable cogging torque mitigation technique, two variants of TFM were realized. This first variant is with rotor modification, to study the effect of remanence of PM and the second variant is with stator modification, to study the impact of the introduction of the square and trapezoidal shunt. The realized motor hardware units and the assembled motor are shown in Figure 16. 49% cobalt-steel alloy is used as the stator and rotor material for the motor. Fabrication is carried out using wire cut electrical discharge machining motor stator and rotor parts are fabricated from 49% cobalt-steel alloy rod by wire cut electrical discharge machining. 28 MGOe Samarium cobalt is used as

a permanent magnet and magnetizer-calibrator assembly is used for magnetizing it to the required level. 25 AWG copper wire is used for stator winding and an automated coil winding machine is used for winding.
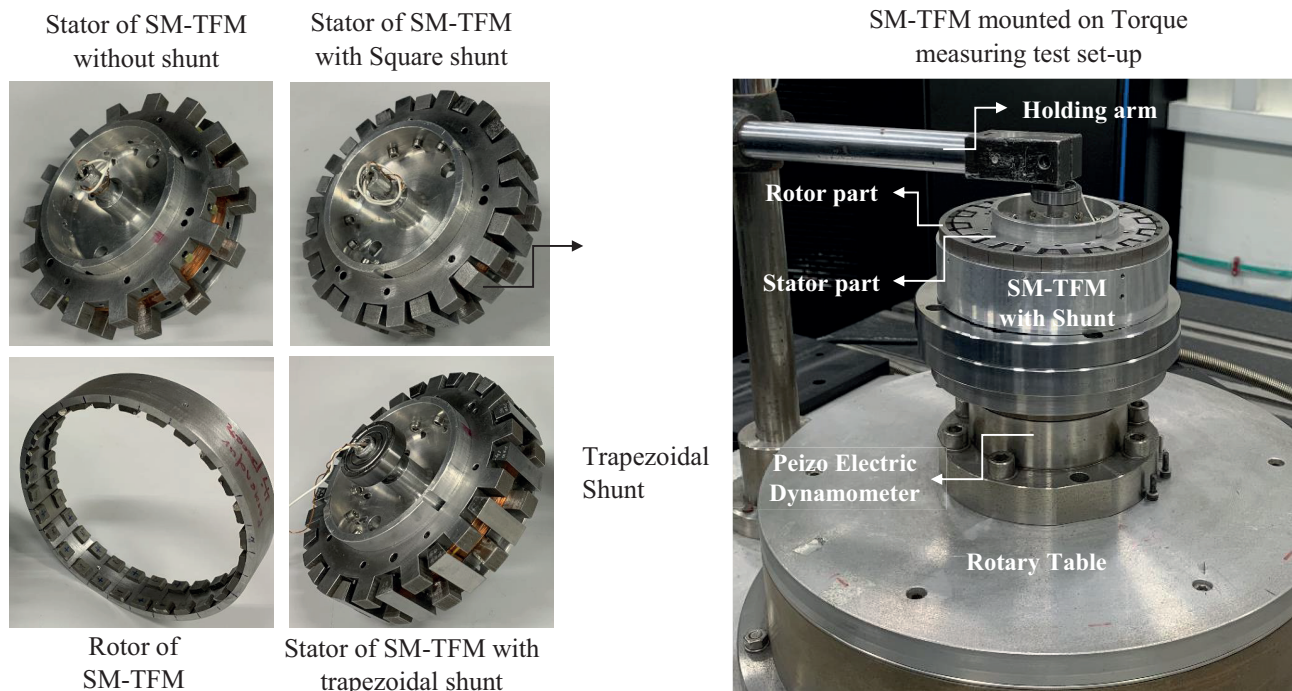

Figure 16. Hardware components and the torque measurement test setup of SM-TFM

4.1. Experimental setup and torque measurement

The developed torque of the realized single stack TFM is measured with an experimental set-up as shown in Figure 16. It consists of a piezoelectric dynamo-meter/charge amplifier for measuring torque, a computerized rotating table and an automated data acquisition system. Here the rotor was held firmly and the stator was rotated continuously at the rate of $1°/s$. Electromagnetic torque is measured by giving DC excitation to the winding and the cogging torque is measured without giving excitation. The electromagnetic and cogging torque patterns were taken for one pole-pitch.

4.2. Effect of remanence of permanent magnet

Samarium cobalt which possesses better thermal stability with an energy product of 28 MGOe is used as the permanent magnet in both rotors. The magnetic circuit of the motor which contains hard and soft magnetic material, and airgap of the motor decide the operating point of the motor. Change in the remanence of the magnet changes the operating point of PM. The remanence of the PM can be changed while magnetization by changing the magnetizing voltage. Two 28 poles rotors for TFM were realized, one with PM having the remanence of 1.00 Tesla and the other with 0.6 Tesla. The variation of the peak cogging torque and average electromagnetic torque for different excitation is shown in Figure 17. It is observed that till the excitation of 2A, developed torque varies linearly. Beyond 2A, there is a decrease in the slope which points out the material saturation. The torque constant of the machine with low power magnet and high power magnet till 2A of excitation is 1.00 Nm/A and 1.75 Nm/A, respectively.
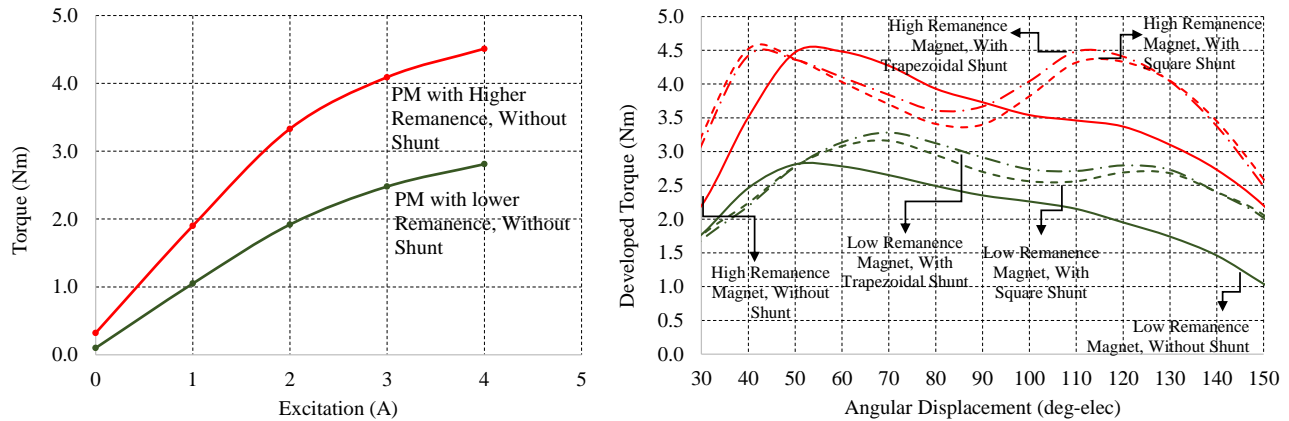
Figure 17. Variation of developed torque with excitation for SM-TFM with low power and high power magnet rotor.

4.3. Effect of shunt

Developed torque pattern was taken for the SM-TFM without and with square shunt & trapezoidal shunt stator with the rotor combination of high and low power magnets and shown in Figure 17. It is observed that with the introduction of the shunt, the peak of the second half of the developed torque pattern increased. The torque pattern of TFM with a square and trapezoidal shunt is near identical. The performance parameters are tabulated in Table 5. It is observed that the usage of low remanence magnets in place of high remanence magnets in the rotor reduces the cogging torque by 69% with a 40% reduction in the developed torque. In this case, torque ripple increases by 27%. With the introduction of shunt, even though cogging torque increases by 21%, torque ripple reduces by 22 % with 7% increases in the developed torque. This proportion is near-identical also to low power magnet rotor. Developed torque is maximum for trapezoidal shunt stator with high remanence rotor.

Table 5. Comparison of various mitigation techniques on the performance parameters of TFM.

Parameter	Rotor with high remanence PM			Rotor with low remanence PM		
	Cogging Torque (Norm)	Developed Torque (Norm)	Torque Ripple ((Norm)	Cogging Torque (Norm)	Developed Torque (Norm)	Torque Ripple (Norm)
Stator without shunt	0.19	1.00	1.00	**0.06**	0.61	1.27
Stator with square shunt	0.23	1.07	**0.78**	0.08	0.75	0.81
Stator with trapezoidal shunt	0.24	**1.09**	0.80	0.09	0.77	0.90

The FE simulation results are fairly matching with the experimental results. The increase in the peak of second half of the developed torque pattern with the introduction of shunt, which is observed during simulation is perfectly reproduced during hardware experiments. An increase in cogging torque with the introduction of square and trapezoidal shunt is observed in both simulation and hardware experiments. By simulation, there is 9% and 17% increase in the developed torque with the introduction of square and trapezoidal shunt respectively, whereas the increase is 7% and 9% during hardware experimentation. The deviation between simulation and hardware test results for developed torque and torque ripple is respectively 7.3% and 5.2% (maximum). With low

remanence rotor, cogging and developed torque are reduced by 71% and 42%, respectively during simulation, whereas the reduction is 69% and 40% while experimentation. The deviation observed between simulation and hardware test results are 4.2% for cogging torque and 6.1% for developed torque. The inaccuracy and discrepancy between the simulation and hardware test results shall be attributed by the complex magnetization pattern in the magnetic circuits, fabrication tolerances and assembly related errors.

5. Conclusion

TFM has complex magnetic field distribution and extensive 3D finite element analysis (FEA) was carried out to characterize the cogging torque which is generated due to the interaction between stator poles and rotor permanent magnets. The effect of basic design variables of SM-TFM namely pole numbers, airgap, magnet thickness, magnet remanence, pole-arc to pole-pitch ratios of stator and rotor poles on the production of cogging torque is discussed. The peak cogging torque varies in a pattern with the pole number whereas the torque ripple is found to increase with the increase in number of poles. A linear relationship is found to exist between the airgap and the electromagnetic torque and on the other hand, it is inverse-square for the cogging torque. When the magnet thickness is 57% of the stator pole thickness, the motor delivers maximum electromagnetic torque and the cogging torque is 0.17 times the electromagnetic torque. Developed torque and torque ripple vary linearly with the remanence except for the initial variation in the torque ripple. The pole-arc to the pole-pitch ratio of the stator and rotor poles has a prominent effect on the developed torque of TFM. Based on the stator and rotor pole-arc, two cases of SM-TFM have been identified and analyzed viz., one with maximum cogging torque and the other with minimum cogging torque.

The conventional cogging torque mitigation techniques used in BLDC and PMSM motors are extensively studied for SM-TFM and its effect on developed torque and torque ripple are analyzed in detail on the identified two cases of SM-TFM. The different methods include skewing of rotor poles, notching of the stator poles, introduction of stator asymmetry, provision of wedges at stator poles, segmentation of the magnets and introduction of shunt. A comparative analysis of these techniques was carried out. Among all the cogging torque mitigation techniques, introduction of trapezoidal shunt has provided an added advantage of an increase in the electromagnetic torque in addition to the decrease in torque ripple with a minimal increase in the cogging torque for both cases of SM-TFM.

To study the effect of cogging torque mitigation techniques, two hardware variants of SM-TFM were realized, one with the modified stator having shunt and the other with the modified rotor having low remanence permanent magnet. It is observed that the SM-TFM with a shunted stator and low remanence magnet is effective with reduced torque ripple in addition to the improved electromagnetic torque. The introduction of the shunt increased the peak of the second half of the developed torque pattern. The usage of low remanence magnets in place of high remanence magnets in the rotor reduces the cogging torque by 69% with a 40% reduction in the developed torque. Hence an SM-TFM with a shunted stator and low remanence magnet is proposed as the best suited drive motor for the direct drive low speed precise position control spacecraft requirement.

References

[1] Selection of electric motors for aerospace applications - NASA Document on Preferred Reliability Practice. pp. 1-6. Practice No. PD-ED-1229.

[2] RP Praveen, MH Ravichandran. A Novel Slotless Halbach-Array Permanent-Magnet Brushless DC Motor for Spacecraft Applications. IEEE Transactions on Industrial Electronics 2012; 59 (9): 3553-3560. doi: 10.1109/TIE.2011.2161058

[3] Roddy D. Satellite Communications. Mc-Graw Hill Publications, 1995.

[4] Zhang BO, Gregor M. A comparison of the transverse, axial and radial flux PM synchronous motors for electric vehicle. In: IEEE International Electric Vehicle Conference; Florence, Italy; 2014. pp. 1-6. doi: 10.1109/IEVC.2014.7056197

[5] Joao S,Garcia D, Mauricio V, Ferreira da Luz. Transverse Flux Machines - What for. IEEE Transactions on Multidisciplinary Engineering Education Magazine 2007; 2 (1): 4-6.

[6] Jordan S, Baker NJ. Air-cooled, high torque machines for aerospace applications. In: 8th IET International Conference on Power Electronics Machines and Drives; Glasgow, UK; 2016. pp. 1-6. doi: 10.1049/cp.2016.0236

[7] Yang X, Kou B. Electromagnetic Design of a Dual-Consequent-Pole Transverse Flux Motor. IEEE Transactions on Energy Conversion 2020; 35 (3): 1547–1557. doi: 10.1109/TEC.2020.2982432

[8] Changpeng LV, Lichun Zhang, Yongxiang Xu. Research on novel high torque density transverse flux permanent magnet motor. In: 22nd International Conference on Electrical Machines and Systems; Harbin, China; 2019. pp. 1-5. doi: 10.1109/ICEMS.2019.8922009

[9] Bheeman V, Nagaratnam S. Effect of Stator permanent magnet thickness and rotor geometry modifications on the minimization of cogging torque of a flux reversal machine. Turkish Journal of Electrical Engineering & Computer Science 2017; 25 (1): 4907-4922. doi: 10.3906/elk-1703-33

[10] Bianchi N, Bolognani S. Design techniques for reducing the cogging torque in surface-mounted PM motors. IEEE Transactions on Industrial Applications 2002; 38 (5): 1259–1265. doi: 10.1109/TIA.2002.802989

[11] Bianchini C, Immovilli F, Lorenzani E, Davoli M. Review of design solutions for internal permanent-magnet machines cogging torque reduction. IEEE Transactions on Magnetics 2012; 48 (10): 2685–2693. doi: 10.1109/TMAG.2012.2199509

[12] Muljadi E,Green J. Cogging torque reduction in a permanent magnet wind turbine generator. In: 21st Mechanical Engineers Wind Energy Symposium of American Society; Reno, Nevada; 2002. pp. 340–342.

[13] Aydin M. Magnet skew in cogging torque minimization of axial gap permanent magnet motors. In: International Conference on Electrical Machines and Systems; Wuhan, China; 2008. pp. 1–6. doi: 10.1109/ICEL-MACH.2008.4799945

[14] Caricchi CF, Capponi FG, Crescimnini F. Experimental study on reducing cogging torque and no-load power loss in axial flux permanent magnet machines with slotted winding. IEEE Transactions on Industrial Applications 2004; 40 (4): 1066-1075. doi: 10.1109/TIA.2004.831273

[15] Dreher F, Parspour M. Reducing the cogging torque on PM transverse flux machines by discrete skewing of a segmented stator. In: 20th International Conference on Electrical Machines; Marseille, France; 2012. pp. 454-457. doi: 10.1109/ICElMach.2012.6349908

[16] Islam R, Husain I,McLaughlin K. Permanent-magnet synchronous motor magnet designs with skewing for torque ripple and cogging torque reduction. IEEE Transactions on Industrial Applications 2009; 45 (1): 152– 160. doi: 10.1109/TIA.2008.2009653

[17] Shao N, Li Zhu. Analytical Methods for Optimal Rotor Step Skewing To Minimize Cogging Torque in Permanent Magnet Motors. In: 22nd International Conference on Electrical Machines and Systems; Harbin, China; 2019. pp. 1-5. doi: 10.1109/ICEMS.2019.8921502

[18] Aydi M, RQR Qu, Lipo TA . Cogging torque minimization technique for multiple-rotor, axial-flux, surface-mounted-PM motors: Alternating magnet pole-arcs in facing rotors. In: 38th IAS Annual Conference; Salt Lake City, UT, USA; 2003. pp. 555-561. doi: 10.1109/IAS.2003.1257555

[19] Kastinger G,Schumacher A. Reducing Torque ripple of transverse flux machines by structural designs. In: IET International Conference on Power Electronics and Drives; Sante Fe, NM, USA; 2002. pp. 320-324. doi: 10.1049/cp:20020136

[20] Lee JY, Chang JH. Tooth shape optimization for cogging torque reduction of transverse flux rotary motor using design of experiment and response methodology. IEEE Transactions on Magnetics 2007; 43 (4): 1817-1820. doi: 10.1109/TMAG.2007.892611

[21] Gonzalez DA, Tapia JA . Design consideration to reduce cogging torque in axial flux permanent-magnet machines. IEEE Transactions on Magnetics 2007; 43 (8): 3435-3440. doi: 10.1109/TMAG.2007.899349

[22] Letelier AB , Gonzalez DA , Tapia JJ . Cogging torque reduction in an axial flux PM machine via stator slot displacement and skewing. IEEE Transactions on Industrial Applications 2007; 43 (3): 685-696. doi: 10.1109/TIA.2007.895738

[23] J Yan, H Lin, ZQ Zhu, P Jin, Y Guo. Cogging torque optimization of flux switching transverse flux permanent magnet machine. IEEE Transactions on Magnetics 2013; 46 (5): 2169-2172. doi: 10.1109/TMAG.2013.2244855

[24] Yasuhito Ueda, Hiroshu Takahashi. Cogging Torque Reduction on Transverse-Flux Motor with Multilevel Skew configuration of Tooths Cores. IEEE Transactions on Magnetics 2019; 55 (7): 1-5. doi: 10.1109/TMAG.2019.2893023

[25] H Ahn, G Jang, D Kang. Reduction of the torque ripple and magnetic force of a rotatory two-phase transverse flux machine using herringbone teeth. IEEE Transactions on Magnetics 2008; 44 (11): 4066–4069. doi: 10.1109/TMAG.2008.2001586

[26] Yubo Yang, Xiuhe Wang. Study of magnet asymmetry for reduction of cogging torque in permanent magnet motors. In: 4th IEEE International Conference on Industrial Electronics and Application; Xi'an, China; 2009. pp. 2325-2328. doi: 10.1109/ICIEA.2009.5138614

[27] C Breton, J Bartolome. Influence of machine symmetry on the reduction of cogging torque in permanent-magnet brushless motors. IEEE Transactions on Magnetics 2000; 36 (5): 3819-3823. doi: 10.1109/20.908386

[28] C Liu, J Zhu, Cogging Torque Minimization of SMC PM Transverse Flux Machines Using Shifted and Unequal-Width Stator Teeth. IEEE Transactions on Applied Superconductivity 2016; 26 (4): 1-4. doi: 10.1109/TASC.2016.2543959

[29] Li Hao, Mingyao Lin, Da Xu, Nian Li, Wei Zhang. Cogging Torque Reduction of Axial-Field Flux-Switching Permanent Magnet Machine by Rotor Tooth Notching. IEEE Transactions on Magnetics 2015; 51 (11): 1-4. doi: 10.1109/TMAG.2015.2453340

[30] .Jin Woo Lee, Hong Seok Kim, Byung Il Kwon, Byung Taek Kim. New Rotor Shape Design for Minimum Torque Ripple of SRM Using FEM. IEEE Transactions on Magnetics 2004; 40 (2): 754-757. doi: 10.1109/TMAG.2004.824803

[31] Ramdane Lateb, Noureddine Takorabet, Farid Meibody-Tabar. Effect of Magnet Segmentation on the Cogging Torque in Surface-Mounted Permanent-Magnet Motors. IEEE Transactions on Magnetics 2006; 42 (3): 442-445. doi: 10.1109/TMAG.2005.862756

[32] O Dobzhanskyi, R Gouws, E Amiri. On the Role of Magnetic Shunts for Increasing Performance of Transverse Flux Machines. IEEE Transactions on Magnetics 2017; 53 (2): 1-8. doi: 10.1109/TMAG.2016.2621047